



Synthesis of magnetic $\text{Fe}_3\text{O}_4@\text{SiO}_2@\text{Cu-Ni-Fe-Cr}$ LDH: an efficient and reusable mesoporous catalyst for reduction and one-pot reductive-acetylation of nitroarenes

Masumeh Gilanizadeh¹ · Behzad Zeynizadeh¹

Received: 3 December 2017 / Accepted: 7 August 2018 / Published online: 14 August 2018
© Iranian Chemical Society 2018

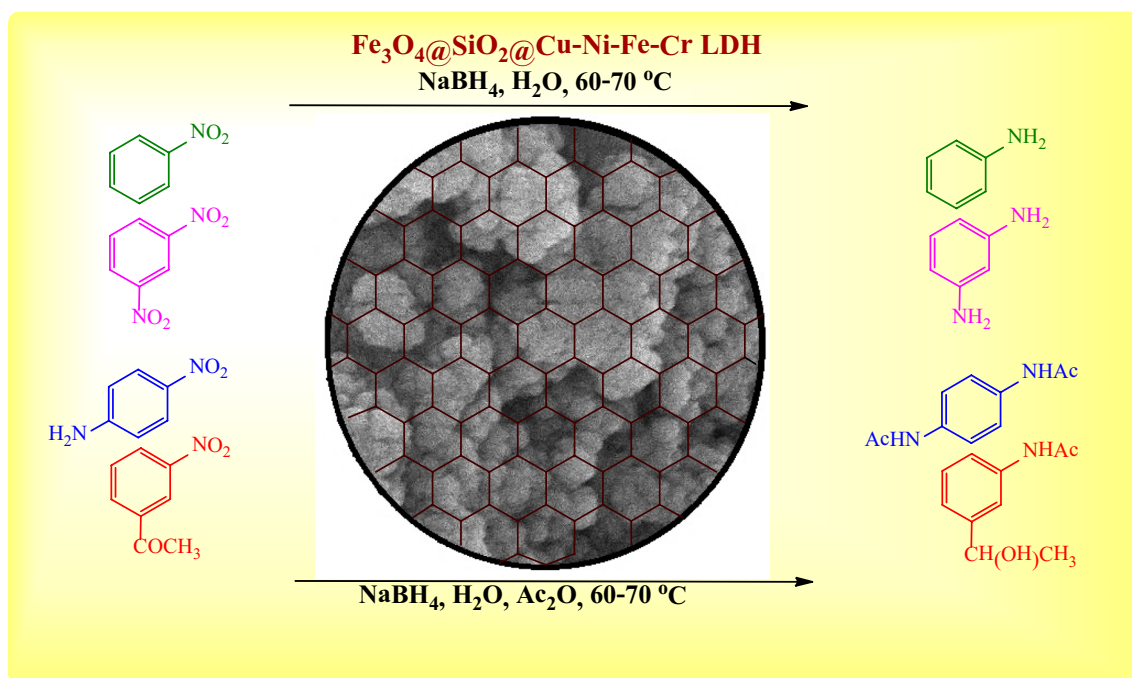
Abstract

Magnetically recoverable $\text{Fe}_3\text{O}_4@\text{SiO}_2@\text{Cu-Ni-Fe-Cr}$ LDH was prepared under co-precipitation conditions. Characterization of the mesoporous catalyst was confirmed using Fourier-transformed infrared spectroscopy, scanning electron microscopy, energy-dispersive X-ray spectroscopy, X-ray diffraction, vibration sample magnetometer, Brunauer–Emmett–Teller, thermogravimetric, differential thermogravimetric analyses and transmission electron microscopy. Reduction of nitroarenes to the corresponding arylamines and one-pot reductive-acetylation of nitroarenes to acetanilides were carried out successfully by nanoparticles of the immobilized Cu–Ni–Fe–Cr layered double hydroxide on silica-coated Fe_3O_4 in water as a green solvent. All reactions were carried out within 6–22 min affording arylamines and *N*-arylacetamides in high-to-excellent yields. Reusability of the core–shell nanocatalyst was examined six times without significant loss of its catalytic activity.

Electronic supplementary material The online version of this article (<https://doi.org/10.1007/s13738-018-1469-x>) contains supplementary material, which is available to authorized users.

Extended author information available on the last page of the article

Graphical abstract



Keywords Arylamines · Acetanilides · $\text{Fe}_3\text{O}_4@\text{SiO}_2@\text{Cu-Ni-Fe-Cr LDH}$ · Nanocatalyst · Reduction · Reductive-acetylation

Introduction

In recent decade, heterogeneous catalysts have become a main part of organic transformations [1–6]. In this context, a number of heterogeneous reagents have been introduced and utilized in synthetic organic chemistry [7–11]. With regard to the mentioned subject, the preparation of magnetically nanoparticles (MNPs) as more efficient heterogeneous catalysts has attracted the attention of scientists owing to their possible abilities and magnetic properties. Magnetite core-shell nano-structure catalysts can be easily separated from the reaction mixture by an external magnetic field to keep away usual filtration procedures [12–14]. Recently, the application of magnetic nanoparticles has been widely documented and numerous procedures have been introduced for the modification of magnetite nanocores by various transition metals as well as other metallic compounds [15–30].

Arylamines are known as important intermediates in the synthesis of various organic compounds such as agricultural chemicals, herbicides, pharmaceuticals, dyes, pigments and photographic materials [31–37]. Generally, aromatic amines are prepared by reduction of nitro compounds and due this, various manuscripts showed the importance of this synthetic protocol [38–45]. In this context, the combination system of

NaBH_4 with metal halides or salts reduces nitro compounds under ordinary conditions. However, in the absence of these additives, the reduction does not take place [46–48].

Protection of functional groups is an essential step in the synthesis of compounds with the complex functionalities. One-pot reductive-acetylation of nitroarenes under demanding conditions is a straightforward method for the preparation of *N*-arylacetamides without isolating the intermediate amines. In contrast, a usual two-step procedure endures practical difficulties during the separation and purification of amines. In this area, various documents show the importance of direct transformation of nitroarenes to *N*-arylacetamides [49–58]. Although most of the reported methods bring useful synthetic advantages, they generally suffer from using expensive organic solvents and reagents, prolonged reaction times, harsh reaction conditions and unsatisfactory yields. Therefore, the development and introduction of a simple method which utilizes mild and effective catalyst as well as using green reaction conditions is still a subject of more interest.

In line with the outlined strategies and continuation of our research programs to the reduction of nitro compounds [59–63], herein, we wish to report $\text{Fe}_3\text{O}_4@\text{SiO}_2@\text{Cu-Ni-Fe-Cr}$ layered double hydroxide, for the first time,

as an efficient and separable nanocatalyst for rapid reduction and reductive-acetylation of various nitroarenes with NaBH_4 in water as a green solvent (Scheme 1).

Results and discussion

Synthesis and characterizations of nanocatalyst

In the present study, we represent the synthesis of nano- $\text{Fe}_3\text{O}_4@/\text{SiO}_2@/\text{Cu-Ni-Fe-Cr}$ LDH through a three-step procedure: (1) preparation of Fe_3O_4 MNPs by a chemical co-precipitation of $\text{FeCl}_3\cdot 6\text{H}_2\text{O}$ and $\text{FeCl}_2\cdot 4\text{H}_2\text{O}$ in NH_4OH , (2) coating of silica layer on the surface of magnetite nanocores by tetraethyl orthosilicate (TEOS) at room temperature (Scheme 2), and (3) addition of Cu-Ni-Fe-Cr LDH on the surface of $\text{Fe}_3\text{O}_4@/\text{SiO}_2$ MNPs via an in situ growth procedure by aqueous solutions of Cu^{2+} , Ni^{2+} , Fe^{3+} and Cr^{3+} salts (Scheme 3).

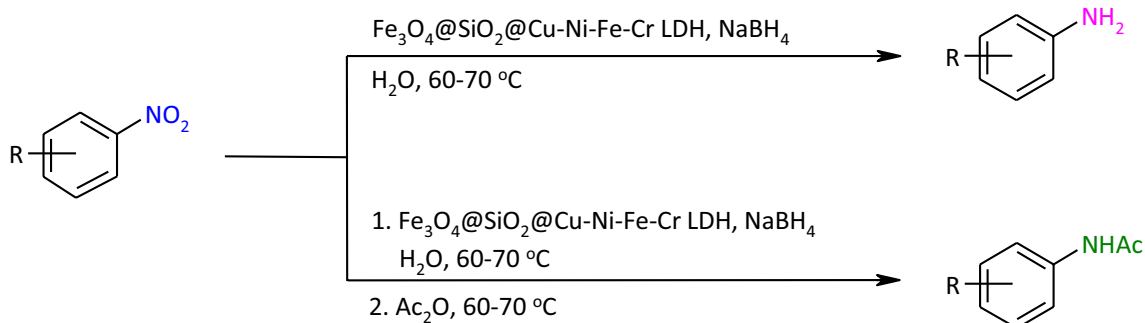
Fourier-transformed infrared spectroscopy (FTIR)

The structure of magnetic nanoparticles of Fe_3O_4 , $\text{Fe}_3\text{O}_4@/\text{SiO}_2$ and $\text{Fe}_3\text{O}_4@/\text{SiO}_2@/\text{Cu-Ni-Fe-Cr}$ LDH was primarily elucidated by their FTIR spectra. The FTIR spectrum of Fe_3O_4 (Fig. 1a) represents a strong absorption peak at 575 cm^{-1} which is related to the vibration of Fe-O bonds in iron oxide. The absorption peaks at 1625 and 3400 cm^{-1} are also assigned to O-H deforming and stretching vibrations of adsorbed water, respectively. In comparison to the spectrum of Fe_3O_4 , additional peaks in FTIR spectrum of

$\text{Fe}_3\text{O}_4@/\text{SiO}_2$ MNPs (Fig. 1b) are observable. The peaks around 796 and 1094 cm^{-1} are attributed to symmetrical and asymmetrical stretching of Si-O-Si . These results exhibited that the silica layer was successfully immobilized on the surface of magnetite nanocores. The FTIR spectrum of nano- $\text{Fe}_3\text{O}_4@/\text{SiO}_2@/\text{Cu-Ni-Fe-Cr}$ LDH (Fig. 1c) shows a strong and broad absorption band around $3300\text{--}3600\text{ cm}^{-1}$ which is related to the superimposition of stretching band of metal hydroxyl groups in the layers and hydrogen-bonded water molecules in the interlayer. An additional absorption band at 1600 cm^{-1} represents the water deformation absorption. The observed peak at 1300 cm^{-1} is attributed to the asymmetric stretching of CO_3^{2-} ions in the interlayer. The absorption peaks around $500\text{--}1000\text{ cm}^{-1}$ are also assigned to the lattice vibration modes of M-O and M-OH .

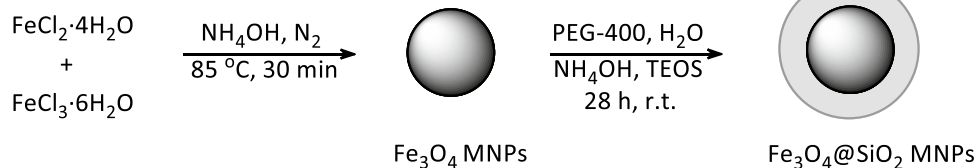
Scanning electron microscopy (SEM)

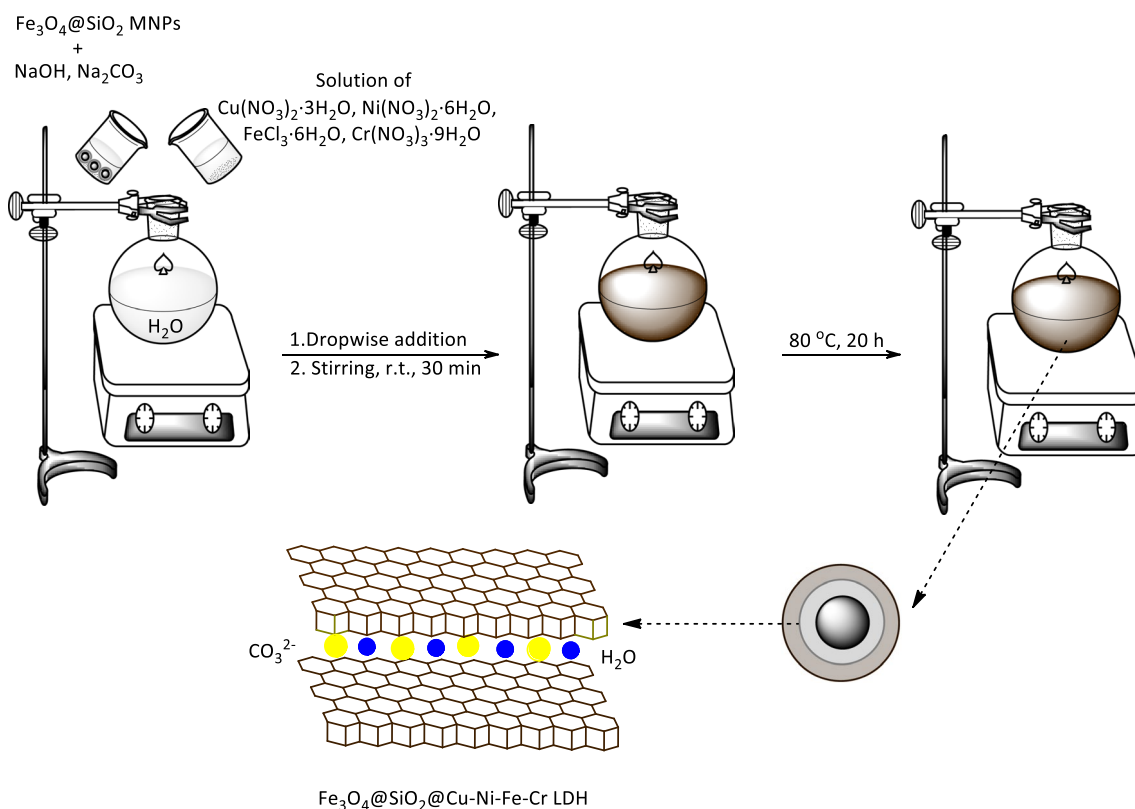
The morphology and size distribution of the synthesized nanocatalyst was determined by scanning electron microscopy technique. SEM images of Fe_3O_4 , $\text{Fe}_3\text{O}_4@/\text{SiO}_2$ and $\text{Fe}_3\text{O}_4@/\text{SiO}_2@/\text{Cu-Ni-Fe-Cr}$ LDH (Fig. 2) show that the catalyst is constructed from roughly spherical and granular nanoparticles. Size distribution of nanoparticles in Fe_3O_4 , $\text{Fe}_3\text{O}_4@/\text{SiO}_2$ and $\text{Fe}_3\text{O}_4@/\text{SiO}_2@/\text{Cu-Ni-Fe-Cr}$ LDH is involved $23\text{--}43\text{ nm}$ (Fig. 2a), $22\text{--}30\text{ nm}$ (Fig. 2b) and $21\text{--}37\text{ nm}$ (Fig. 2c), respectively. According to these distributions, the mesoporous structure of nanocatalyst is approved.



Scheme 1 Reduction and reductive-acetylation of nitroarenes with NaBH_4 /nano-LDH system

Scheme 2 Synthesis of $\text{Fe}_3\text{O}_4@/\text{SiO}_2$ MNPs





Scheme 3 Synthesis of nano- $\text{Fe}_3\text{O}_4@SiO_2@Cu-Ni-Fe-Cr$ LDH

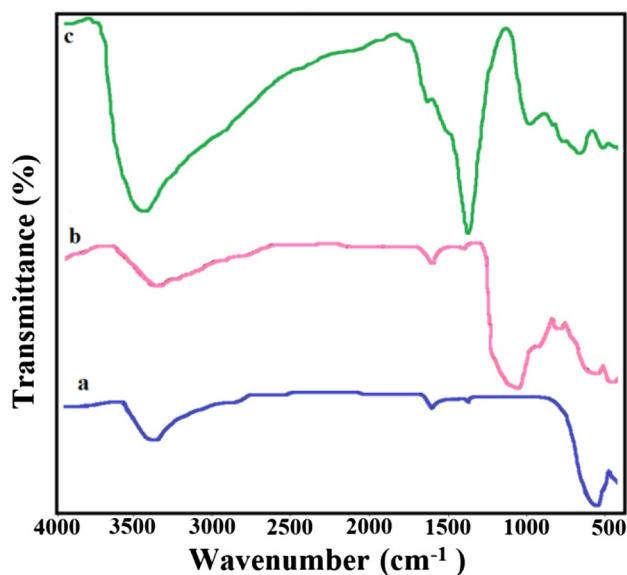


Fig. 1 FTIR spectrum of **a** Fe_3O_4 , **b** $\text{Fe}_3\text{O}_4@SiO_2$ and **c** $\text{Fe}_3\text{O}_4@SiO_2@Cu-Ni-Fe-Cr$ LDH

Energy-dispersive X-ray spectroscopy (EDX)

Electron dispersive analysis (EDX) is a convenient technique for detection of elements in a material. According to the elemental contents and EDX spectrum of Fe_3O_4 (Fig. 3a), $\text{Fe}_3\text{O}_4@SiO_2$ (Fig. 3b) and $\text{Fe}_3\text{O}_4@SiO_2@Cu-Ni-Fe-Cr$ LDH (Fig. 3c), the LDH layer of Cu–Ni–Fe–Cr was successfully immobilized on the surface of $\text{Fe}_3\text{O}_4@SiO_2$ MNPs.

X-ray diffraction (XRD)

X-ray diffraction (XRD) analysis as another tool was also used for structural elucidation of the prepared laboratory samples. Figure 4a represents diffraction peaks at $2\theta = 30.2^\circ$, 35.5° , 43.3° , 53.7° , 57.2° and 62.9° corresponding to (022), (113), (004), (224), (115) and (044) crystal planes of nano- Fe_3O_4 . The pattern has a crystalline cubic spinel structure which is in agreement with the standard one of Fe_3O_4 (JCPDS 65-3107) [64, 65]. Figure 4b shows that in XRD pattern of $\text{Fe}_3\text{O}_4@SiO_2$ MNPs, the same pattern of nano- Fe_3O_4 is also observable describing the embedded magnetite cores keep their crystalline phase after coating of amorphous silica layer. Figure 4c illustrates the XRD pattern of $\text{Fe}_3\text{O}_4@SiO_2@Cu-Ni-Fe-Cr$ LDH. The peaks at $2\theta = 11.49^\circ$, 23.38° , 34.26° , 38.81° , 60.37° and 61.73° are attributed to

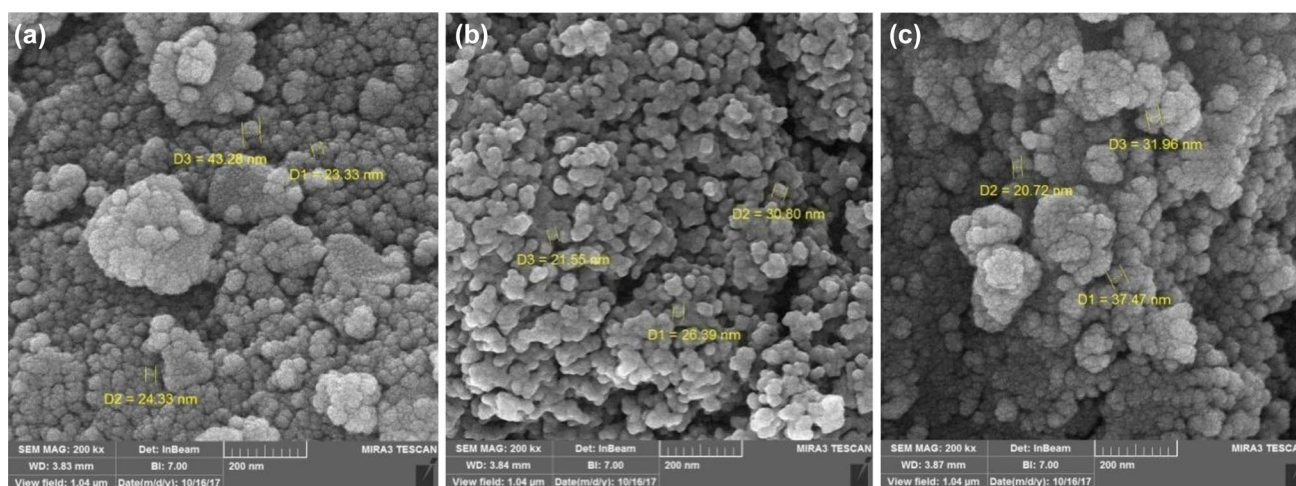


Fig. 2 FE-SEM image of **a** Fe_3O_4 , **b** $\text{Fe}_3\text{O}_4@SiO_2$, and **c** $\text{Fe}_3\text{O}_4@SiO_2@Cu-Ni-Fe-Cr$ LDH

(003), (006), (102), (105), (110) and (113) crystal planes in green rust. The hydroxalcalite has a hexagonal crystal system which is in good agreement with ICSD reference pattern of 00-049-0723 (iron nickel chloride hydroxide hydrate). In addition, it shows a series of sharp and intense symmetric lines peaks at low values of 2θ representing the characteristic structure of hydroxalcalite-like materials [66]. Strong peaks related to (003) and (006) planes were observed and the angle of the peak of (003) indicated large distance between interlayers.

Vibration sample magnetometer (VSM)

Magnetic characterization of the prepared samples is depicted in Fig. 5. The curves represent reversible and non-linear saturation magnetization (M_s) value of Fe_3O_4 (70 emu g^{-1}) (Fig. 5a), $\text{Fe}_3\text{O}_4@SiO_2$ (30 emu g^{-1}) (Fig. 5b) and $\text{Fe}_3\text{O}_4@SiO_2@Cu-Ni-Fe-Cr$ LDH (6 emu g^{-1}) (Fig. 5c). The graphs clearly show that during the immobilization of one-shell around the other one, the saturation magnetization (M_s) value is intensively decreased.

Brunauer–Emmett–Teller (BET)

BET and BJH methods were applied to study the surface area and pore size distribution of the nanocatalyst. The nitrogen adsorption and desorption isotherms of the prepared $\text{Fe}_3\text{O}_4@SiO_2@Cu-Ni-Fe-Cr$ LDH are shown in Fig. 6. The calculated specific surface area using BET was $42.087 \text{ m}^2\text{g}^{-1}$. The pore volume was $0.0712 \text{ cm}^3\text{g}^{-1}$. The average pore size of the catalyst was determined 6.8 nm using Barrett–Joyner–Halenda (BJH) method. This confirms the mesoporous structure of the prepared LDH ($2 < D_v < 50 \text{ nm}$).

Thermogravimetric analysis (TGA)

Thermogravimetric analysis as another technique was used to explain the thermal behavior, a possible thermal stability and degradation processes of the synthesized nano-LDH catalyst. According to the depicted TGA-thermograph of Fig. 7a, nano-magnetite has a high thermal stability. At this thermograph, only one thermal degradation step was determined at lower than 45°C . It represents a mass loss of 1.71% due removing of adsorbed-solvent on the surface of magnetite nanocores. Figures 7b and 8a show the TGA and DTG thermograph of $\text{Fe}_3\text{O}_4@SiO_2$ MNPs with two thermal degradation steps. The first decomposition step (mass loss of 2.18%) is related to removing of adsorbed water or solvent in a range of $30\text{--}158^\circ\text{C}$. The weight loss (3.28%) at the second degradation step occurred in the range of $474\text{--}616^\circ\text{C}$. The sum of these two degradation steps gives a direct confirmation for loading of silica layer on the surface of magnetite nanocores. As well, the TGA and DTG thermograph of $\text{Fe}_3\text{O}_4@SiO_2@Cu-Ni-Fe-Cr$ LDH (Figs. 7c, 8b) represent two thermal degradation steps. The first weight loss (11.98%) was identified in the range of $170\text{--}275^\circ\text{C}$ showing the elimination of water from the interlayer and surface area. The second weight loss (15.12%) in the range of $275\text{--}395^\circ\text{C}$ is also attributed to dehydroxylation of layers and loss of CO_3^{2-} from interlayer.

Transmission electron microscopy (TEM)

The transmission electron microscope (TEM) images of nano- $\text{Fe}_3\text{O}_4@SiO_2@Cu-Ni-Fe-Cr$ LDH shows that the nanocatalyst has a core-shell structure (Fig. 9).

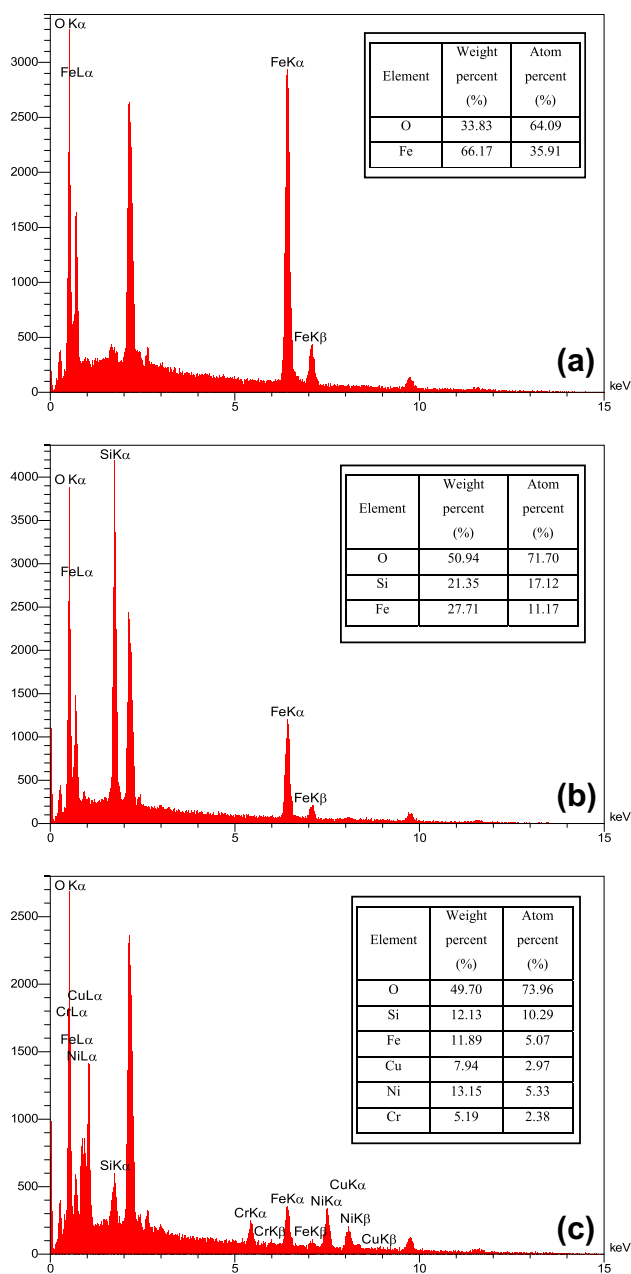


Fig. 3 EDX and elemental contents of **a** Fe_3O_4 , **b** $\text{Fe}_3\text{O}_4@SiO_2$, and **c** $\text{Fe}_3\text{O}_4@SiO_2@Cu-Ni-Fe-Cr$ LDH

Catalytic reduction and one-pot reductive-acetylation of aromatic nitro compounds with NaBH_4

After the successful synthesis and characterization of nano- $\text{Fe}_3\text{O}_4@SiO_2@Cu-Ni-Fe-Cr$ LDH, in continuation, catalytic activity of the prepared nano-LDH towards reduction of nitro compounds was studied. In this context, reduction of nitrobenzene as a model compound with NaBH_4 in the presence of nano-LDH under diverse reaction conditions was

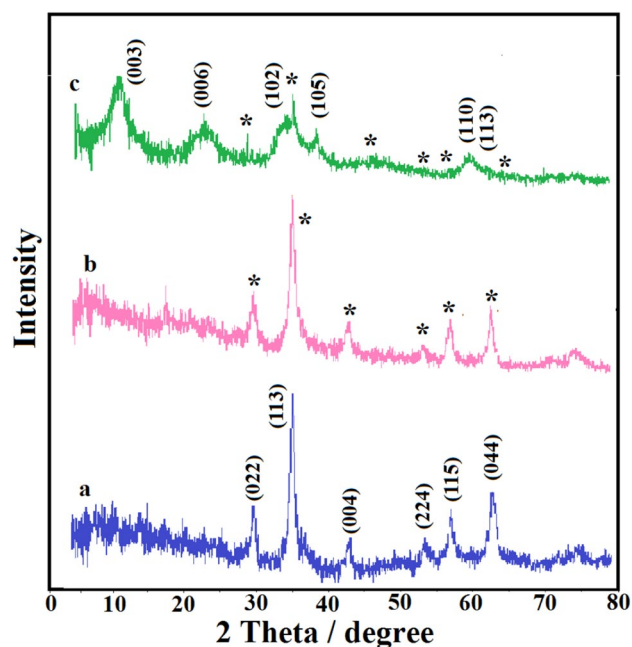


Fig. 4 XRD pattern of **a** Fe_3O_4 , **b** $\text{Fe}_3\text{O}_4@SiO_2$ and **c** $\text{Fe}_3\text{O}_4@SiO_2@Cu-Ni-Fe-Cr$ LDH

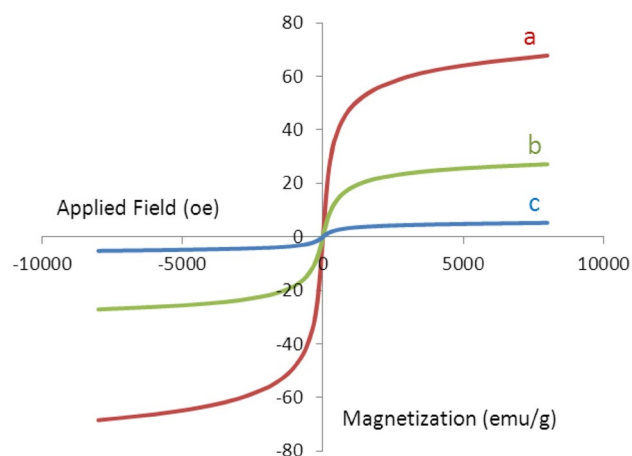


Fig. 5 Magnetization curve of **a** Fe_3O_4 , **b** $\text{Fe}_3\text{O}_4@SiO_2$, and **c** $\text{Fe}_3\text{O}_4@SiO_2@Cu-Ni-Fe-Cr$ LDH

investigated. The summarized results in Table 1 show that H_2O as a green solvent represents a more efficient influence on the rate of reduction, and therefore it was selected as a solvent of choice. The examinations also exhibited that at the best optimal reaction conditions, the reduction of nitrobenzene (1 mmol) was carried with 2 mmol NaBH_4 in water (2 mL) in the presence of 10 mg of nanocatalyst under oil bath conditions (60–70 °C). In this criterion, aniline was obtained as a sole product within 8 min (Table 1, entry 11).

Encouraged by the success, reduction of various nitroarenes containing electron-withdrawing and releasing

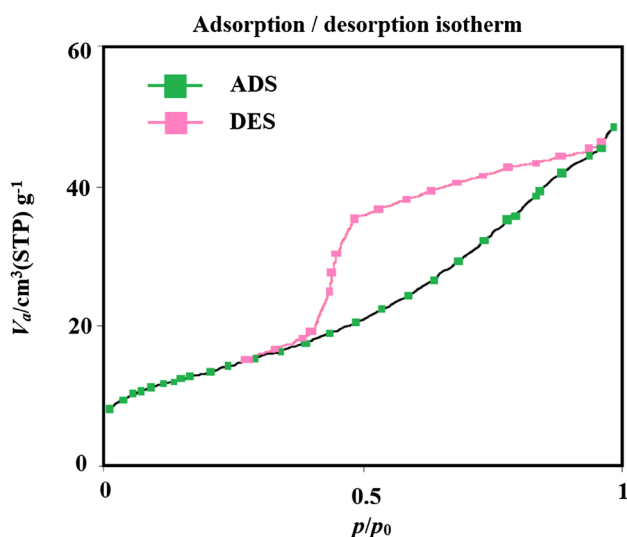


Fig. 6 Nitrogen adsorption–desorption isotherm of $\text{Fe}_3\text{O}_4@\text{SiO}_2@\text{Cu-Ni-Fe-Cr LDH}$

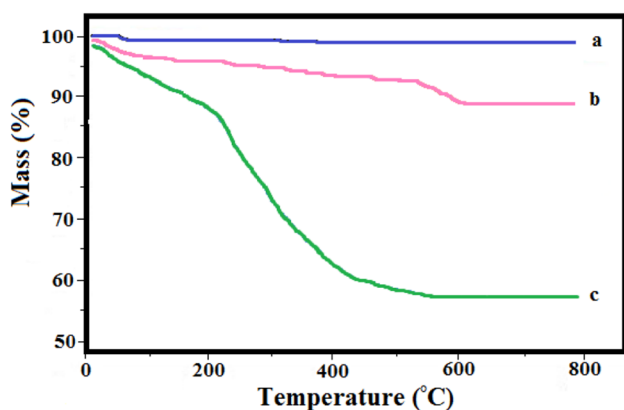


Fig. 7 TGA-thermograph of **a** Fe_3O_4 , **b** $\text{Fe}_3\text{O}_4@\text{SiO}_2$ and **c** $\text{Fe}_3\text{O}_4@\text{SiO}_2@\text{Cu-Ni-Fe-Cr LDH}$

groups was studied at the optimized reaction conditions. The summarized results in Table 2 show that in all cases, the expected products were obtained in high yields. Moreover, the table shows that reduction of nitro compounds containing carbonyl moiety was carried out selectively based on the using amounts of NaBH_4 (Table 2, entries 16–24). The exemplified results represent that a chemoselective reduction of carbonyl group in the presence of nitro moiety can be accessible when lower amounts of NaBH_4 were used. Applying more quantities of NaBH_4 reduces both of nitro and carbonyl groups with the same reactivity. The examination also showed that reduction of 1,3-dinitrobenzene was carried out successfully at the optimized reaction conditions to afford *m*-phenylenediamine in 96% yield (Table 2, entry 15).

The suitability of this synthetic method was shown by comparison of the obtained result for reduction of nitrobenzene by $\text{NaBH}_4/\text{nano-Fe}_3\text{O}_4@\text{SiO}_2@\text{Cu-Ni-Fe-Cr LDH}$ with a number of reported promoters (Table 3). The current study represents advantages in terms of recoverability and reusability combined with satisfactory yields and reaction times.

After the successful reduction of aromatic nitro compounds to arylamines with $\text{NaBH}_4/\text{nano-Fe}_3\text{O}_4@\text{SiO}_2@\text{Cu-Ni-Fe-Cr LDH}$ system, we prompted to investigate the suitability of this synthetic method towards one-pot reductive-acetylation of nitroarenes with acetic anhydride. The issue was investigated by adding Ac_2O to the reaction mixture after reduction of nitrobenzene without isolating the product aniline. The examinations showed that using 1 mmol of Ac_2O per 1 mmol of nitrobenzene was sufficient to complete acetylation of the prepared aniline to the corresponding acetanilide within 1 min under oil bath conditions (60–70 °C). At the optimized reaction conditions, one-pot reductive-acetylation of diverse aromatic nitro compounds to the corresponding acetanilides was carried out successfully by adding Ac_2O (1 mmol) to the reaction mixture after completion of the reductions to the corresponding aniline products. The results of this investigation are shown in Table 4. The table shows that acetylation of amino groups in all aniline products were carried out successfully within 1 min under oil bath conditions. It is notable that in the case of dinitroarenes or aminonitroarenes, acetylation of both of the prepared amino groups was carried out with 2 molar equivalents of Ac_2O (Table 4, entries 2 and 10). In the case of nitro compounds containing carbonyl moiety, acetylation of amino and alcoholic groups was carried out with the chemoselective acetylation of aniline functionality using 1 mmol of Ac_2O . All attempts to perform the acetylation of alcoholic moiety using higher amounts of Ac_2O were unsatisfactory (Table 4, entries 11 and 13).

In order to determine catalytic activity of $\text{nano-Fe}_3\text{O}_4@\text{SiO}_2@\text{Cu-Ni-Fe-Cr LDH}$ towards acetylation of commercially aniline compounds, we also examined the acetylation of aniline with Ac_2O in the presence of nano-LDH. In this case again the reaction was carried out successfully to afford acetanilide in 1 min showing the perfect catalytic activity of $\text{nano-Fe}_3\text{O}_4@\text{SiO}_2@\text{Cu-Ni-Fe-Cr LDH}$ towards the titled transformation.

Although the exact mechanism of these synthetic protocols is not clear, a depicted plausible mechanism in Scheme 4 could be shown the role of $\text{nano-Fe}_3\text{O}_4@\text{SiO}_2@\text{Cu-Ni-Fe-Cr LDH}$ in reduction and one-pot reductive-acetylation of nitroarenes. The scheme represents that through the absorption of hydrogen on the surface of LDH-nanocores, reduction of nitroarenes to arylamines was taken place. In next step and through the activation of acetic anhydride by LDH, nucleophilic attack of the prepared

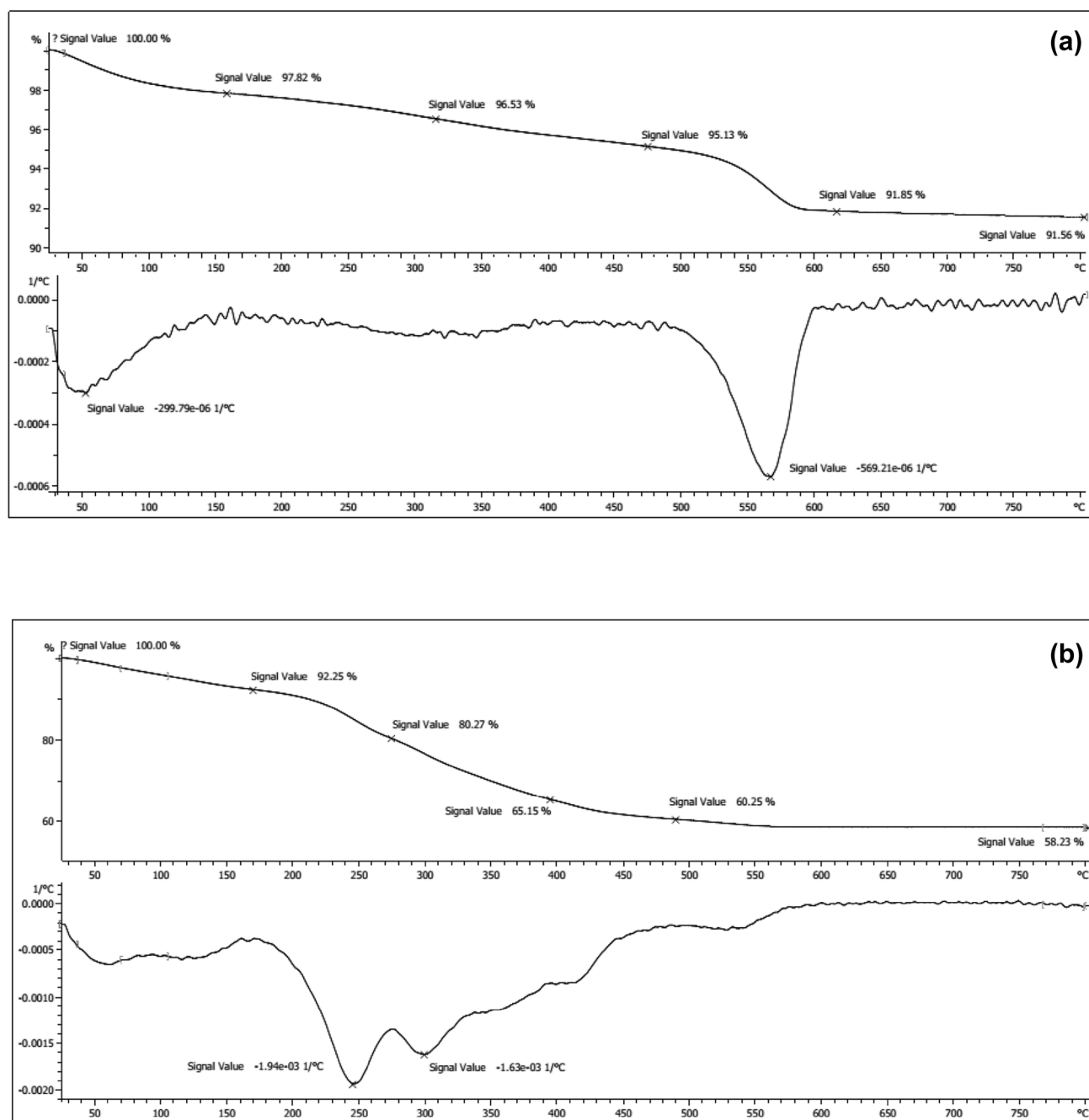


Fig. 8 TGA and DTG thermograph of **a** $\text{Fe}_3\text{O}_4@SiO_2$ and **b** $\text{Fe}_3\text{O}_4@SiO_2@Cu-Ni-Fe-Cr$ LDH

arylamines towards Ac_2O , produces *N*-arylacetamides as final products.

Recycling of $\text{Fe}_3\text{O}_4@SiO_2@Cu-Ni-Fe-Cr$ LDH

In order to study more green and economical aspects of the current protocols, the reusability of nano- $\text{Fe}_3\text{O}_4@SiO_2@Cu-Ni-Fe-Cr$ LDH was also examined by performing reduction and reductive-acetylation of nitrobenzene at

the optimized reaction conditions (Table 2: entry 1 and Table 4: entry 1). After completion of the reactions, the nanocatalyst was separated by an external magnetic field, washed with EtOAc, dried and reused six consecutive cycles without remarkable loss of its activity. The results of these investigations are summarized in Fig. 10.

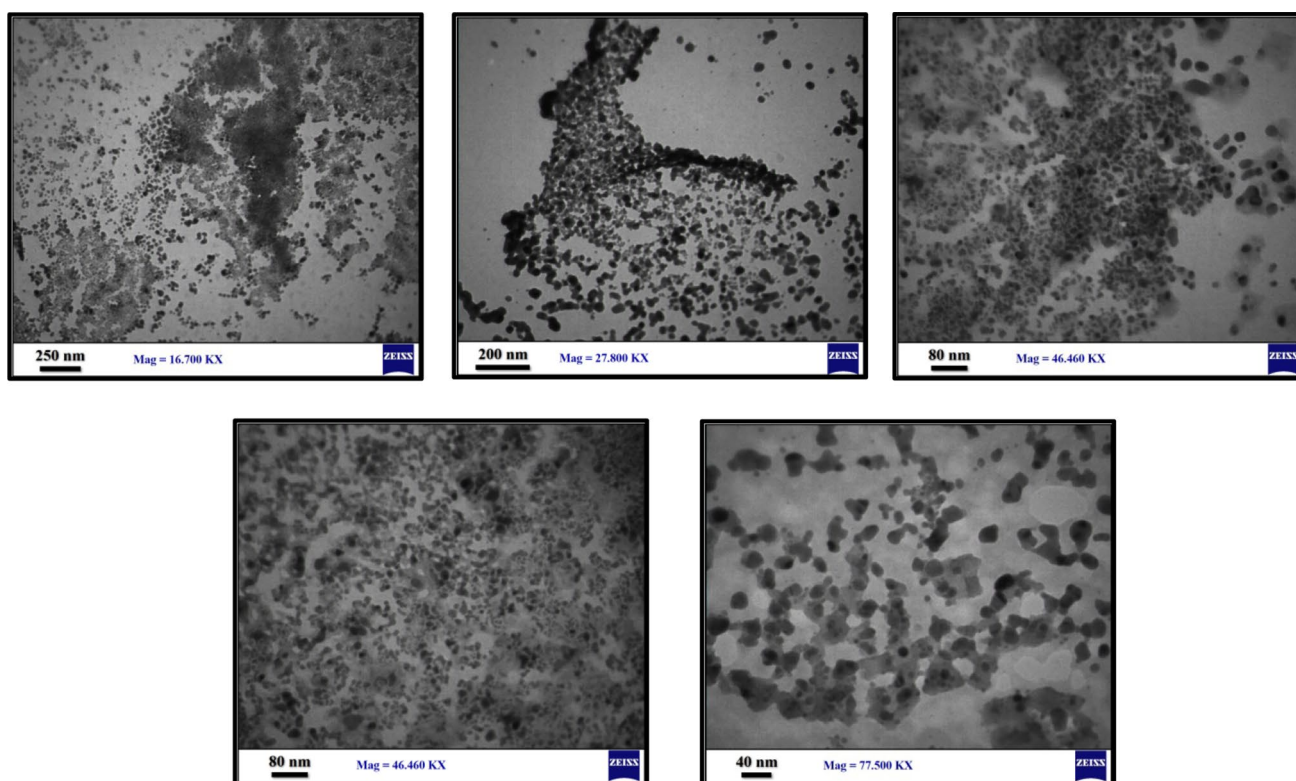


Fig. 9 TEM images of $\text{Fe}_3\text{O}_4@\text{SiO}_2@\text{Cu-Ni-Fe-Cr}$ LDH

Table 1 Optimization experiments for reduction of nitrobenzene to aniline with $\text{NaBH}_4/\text{nano-Fe}_3\text{O}_4@\text{SiO}_2@\text{Cu-Ni-Fe-Cr}$ LDH system under different reaction conditions

Entry	NaBH_4 (mmol)	LDH (g)	Solvent (mL)	Temperature ($^\circ\text{C}$)	Time (min)	Conversion (%)
1	2	–	H_2O	60–70	300	30
2	–	0.1	H_2O	60–70	180	0
3	3	0.1	H_2O	60–70	7	100
4	3	0.1	H_2O	r.t.	40	95
5	3	0.1	EtOH	60–70	75	10
6	3	0.1	CH_3CN	60–70	75	20
7	3	0.1	MeOH	60–70	75	10
8	2	0.1	H_2O	50	20	90
9	2	0.1	H_2O	60–70	6	100
10	2	0.02	H_2O	60–70	8	100
11	2	0.01	H_2O	60–70	8	100
12	2	0.001	H_2O	60–70	20	95

All reactions were carried out with 1 mmol of nitrobenzene in 2 mL solvent

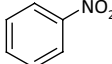
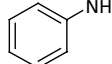
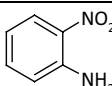
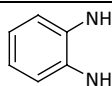
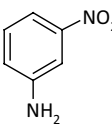
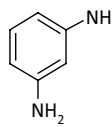
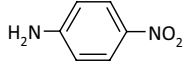
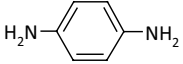
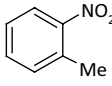
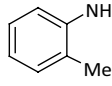
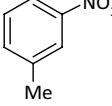
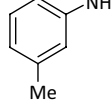

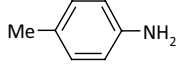
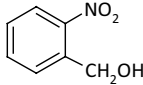
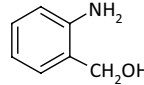
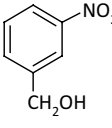
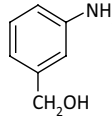
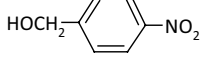
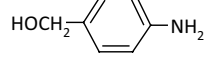
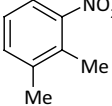
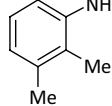
In addition, analysis of the obtained FTIR spectrum (Fig. 11) and SEM images (Fig. 12) of the recycled LDH nanocatalyst after second recycling shows that the structure of nanocatalyst as well as its reactivity remained intact.

Experimental

General

All substrates were purchased from Merck and Aldrich Chemical Companies and they were used without further purification. FTIR and $^1\text{H}/^{13}\text{C}$ NMR spectra were obtained

Table 2 Reduction of nitroarenes with $\text{NaBH}_4/\text{nano-Fe}_3\text{O}_4@\text{SiO}_2@\text{Cu-Ni-Fe-Cr LDH}$ system

Entry	Substrate	Product	Molar ratio Subs./ NaBH_4	LDH (g)	Time (min)	Yield (%) ^b	Ref.
1			1:2	0.01	8	95	[61]
2			1:2	0.01	13	91	[61]
3			1:2	0.01	13	92	[61]
4			1:2	0.01	9	93	[61]
5			1:2	0.01	7	95	[62]
6			1:2	0.01	9	94	[62]
7			1:2	0.01	8	95	[62]
8			1:2	0.01	22	91	[62]
9			1:2	0.01	22	93	[62]
10			1:2	0.01	20	92	[62]
11			1:2	0.02	8	95	[61]

by Thermo Nicolet Nexus 670 and Bruker Avance spectrometers (300 MHz), respectively. TLC was used for the purity determination of the substrates, products and reaction monitoring over silica gel 60 F₂₅₄ aluminum sheet.

Morphology of the particles was examined by measuring SEM using FESEM-TESCAN. The chemical composition of the nanocatalyst was determined by EDX through the SEM analysis. X-ray diffractions (XRD) were made

Table 2 (continued)

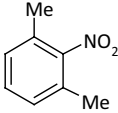
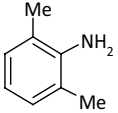
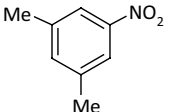
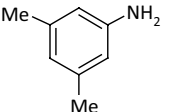
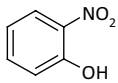
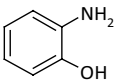
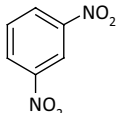
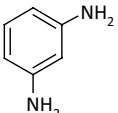
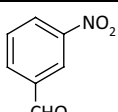
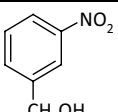
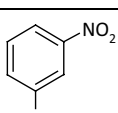
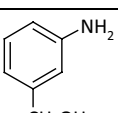
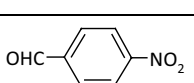
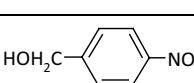
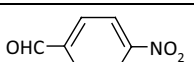
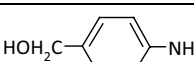
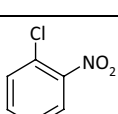
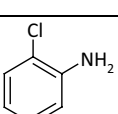
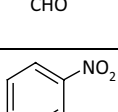
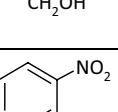
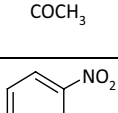
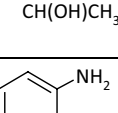
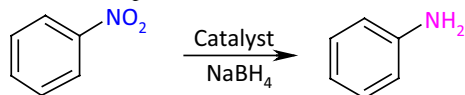
12			1:2	0.02	10	93	[61]
13			1:2	0.02	10	93	[61]
14			1:2	0.04	20	91	[62]
15			1:4	0.01	17	96	[62]
16			1:0.3	0.01	6	95	–
17			1:3	0.01	20	91	[61]
18			1:0.3	0.01	6	95	–
19			1:3	0.01	17	93	[61]
20			1:4	0.02	20	91	[62]
21			1:1	0.01	6	96	–
22			1:3	0.01	18	94	[61]

Table 2 (continued)

23			1:1	0.01	6	93	–
24			1:3	0.01	16	89	[61]
25			1:2	0.01	11	97	[61]

All reactions were carried out in H₂O (2 mL, 60–70 °C)

^aYields refer to isolated pure products

Table 3 Comparison of the reduction of nitrobenzene with NaBH₄/nano-Fe₃O₄@SiO₂@Cu–Ni–Fe–Cr LDH and other reported systems

Entry	Catalyst	Reducing agent	Temperature (°C)	Time (min)	Yield (%)	Reusability (times)	References
1	Fe ₃ O ₄ @SiO ₂ @Cu–Ni–Fe–Cr LDH (10 mg)	NaBH ₄ (2 mmol)	60–70	8	95	6	–
2	Fe ₃ O ₄ @Cu(OH) _x (20 mg)	NaBH ₄ (2 mmol)	55–60	3	95	9	[61]
3	NiFe ₂ O ₄ @Cu (150 mg)	NaBH ₄ (2.5 mmol)	Reflux	1	95	7	[62]
4	Fe ₃ O ₄ @Ni (33 mg)	NaBH ₄ (4 mmol)	r.t.	25	95	30	[42]
5	Fe ₃ O ₄ @Ni (50 mg)	Glycerol/KOH (2 mmol)	80	180	94	8	[43]
6	Nano-Co (11 mg)	N ₂ H ₄ ·2H ₂ O (0.2 mL)	r.t.	300	50	5	[44]
7	Nano-Ni (11 mg)	N ₂ H ₄ ·2H ₂ O (0.2 mL)	r.t.	75	99	5	[44]
8	Co ₃ O ₄ -NGr/C (20 mg)	Formic acid (3.5 mmol)	100	15 h	96	6	[45]

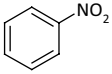
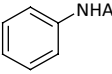
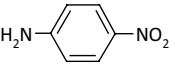
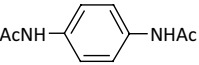
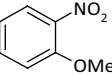
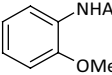
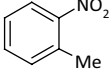
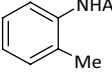
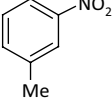
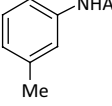
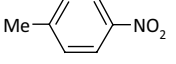
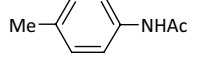
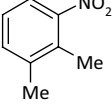
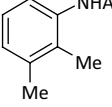
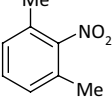
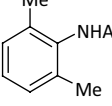
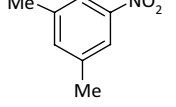
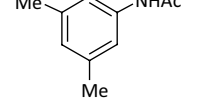
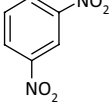
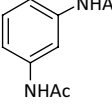
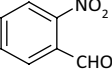
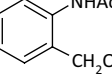
by X'Pert Pro instrument. The X-ray wavelength was 1.5418 Å and the diffraction patterns were recorded in a range of $2\theta = 5^\circ$ – 80° . Magnetic properties of the samples were obtained by a vibration sample magnetometer (VSM, model MDKFT). The N₂ adsorption–desorption isotherms was tested on Belsorp-mini, BET Japan. The specific surface area of sample was measured by the Brunauer–Emmett–Teller (BET) technique. The pore volume and pore size distribution were resulted from the desorption profiles of the isotherms using the Barrett–Joyner–Halenda (BJH) method. Thermogravimetric analyses (TGA) were carried out on STA of Rheometric Scientific Inc.

Preparation of nano-Fe₃O₄@SiO₂@Cu–Ni–Fe–Cr LDH

Preparation of Fe₃O₄ MNPs

Magnetically nanoparticles of Fe₃O₄ were synthesized according to the reported procedure by a chemical coprecipitation of chloride salts of Fe³⁺ and Fe²⁺ [68]. Generally, FeCl₃·6H₂O (5.838 g, 0.0216 mol) and FeCl₂·4H₂O (2.147 g, 0.0108 mol) were dissolved in distilled water (100 mL). The solution was stirred for 10 min at 85 °C under N₂ atmosphere. By the addition of aqueous ammonia (25 wt%, 10 mL) to the resulting solution at 85 °C, nanoparticles of Fe₃O₄ were precipitated immediately. The resulting mixture was stirred at 85 °C under N₂ atmosphere

Table 4 Reductive-acetylation of nitroarenes with $\text{NaBH}_4/\text{Fe}_3\text{O}_4@\text{SiO}_2@\text{Cu-Ni-Fe-Cr}$ LDH system

Entry	Substrate	Product	Molar ratio Subs./ $\text{NaBH}_4/\text{Ac}_2\text{O}$	LDH (g)	Time (min)	Yield (%) ^b	Ref.
1			1:2:1	0.01	9	96	[63]
2			1:2:2	0.01	10	93	[63]
3			1:2:1	0.01	9	91	[67]
4			1:2:1	0.01	8	95	[67]
5			1:2:1	0.01	10	94	[63]
6			1:2:1	0.01	9	95	[67]
7			1:2:1	0.02	9	94	[63]
8			1:2:1	0.02	11	93	[63]
9			1:2:1	0.02	11	93	[63]
10			1:4:2	0.01	18	96	–
11			1:3:2	0.01	21	91	[67]

for 30 min followed by cooling to the room temperature. Nanoparticles of Fe_3O_4 were magnetically separated and washed two times with distilled water and a solution of NaCl (0.02 M).

Synthesis of nano- $\text{Fe}_3\text{O}_4@\text{SiO}_2$ MNPs

The silica layer was coated on the surface of magnetite nanocores according to the reported procedure [69]. Fe_3O_4 (1.5 g)

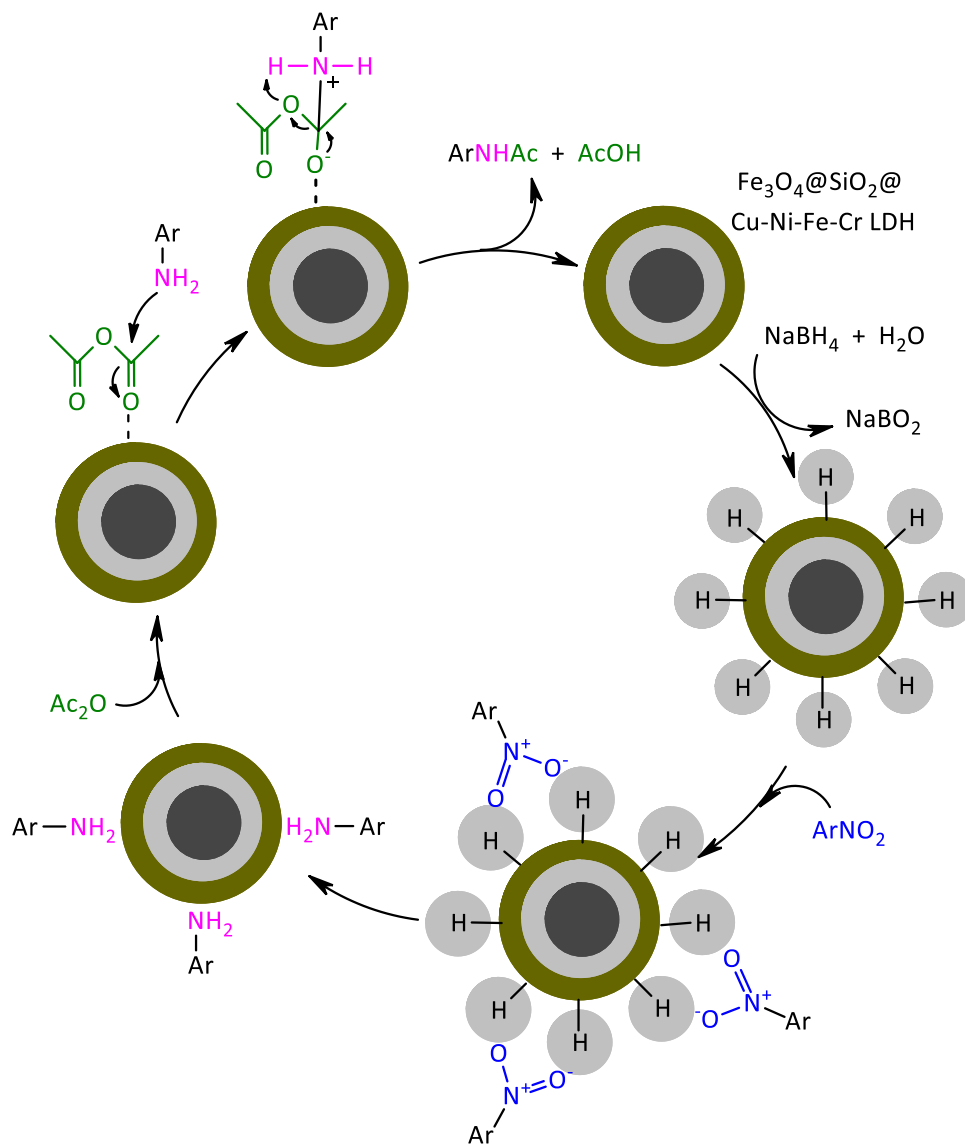
Table 4 (continued)

12			1:2:1	0.01	8	94	[63]
13			1:3:2	0.01	19	94	[67]

All reactions were carried out in H₂O (2 mL, 60–70 °C)

^aYields refer to isolated pure products

Scheme 4 A plausible mechanism for reduction and reductive-acetylation of nitroarenes with NaBH₄/nano-LDH system



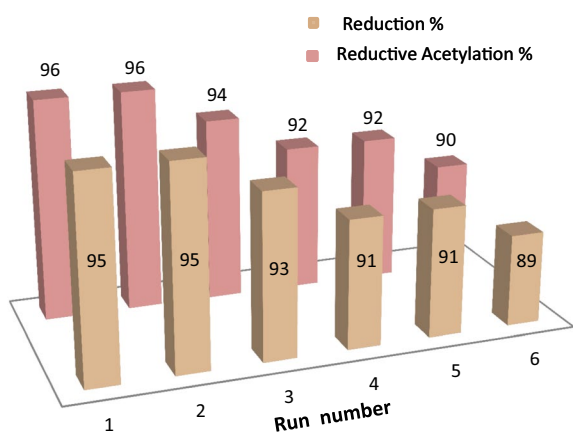


Fig. 10 Recycling of nano- $\text{Fe}_3\text{O}_4@SiO_2@Cu-Ni-Fe-Cr$ LDH in reduction and reductive-acetylation of PhNO_2

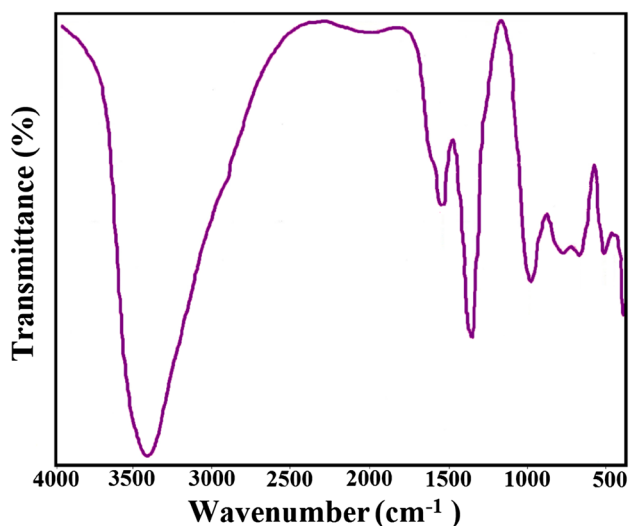


Fig. 11 FTIR spectrum of the recovered $\text{Fe}_3\text{O}_4@SiO_2@Cu-Ni-Fe-Cr$ LDH after second run

was dissolved in distilled water (20 mL), the suspension was added to 2-propanol (200 mL) and then homogenized for 30 min by sonication. Under continuous stirring, PEG-400 (5.36 g), distilled water (20 mL), aqueous NH_4OH (28 wt%, 10 mL) and TEOS (2 mL) were added sequentially into the suspension and the resulting mixture was stirred at room temperature for 28 h. After completion of reaction, the product was separated by an external magnet and washed with ethanol and distilled water.

Synthesis of $\text{Fe}_3\text{O}_4@SiO_2@Cu-Ni-Fe-Cr$ LDH

For the preparation of nano- $\text{Fe}_3\text{O}_4@SiO_2@Cu-Ni-Fe-Cr$ LDH, we have used an in situ growth method for the immobilization of mesoporous Cu-Ni-Fe-Cr LDH on the surface

of $\text{Fe}_3\text{O}_4@SiO_2$ MNPs. Typically, $\text{Fe}_3\text{O}_4@SiO_2$ (0.25 g), Na_2CO_3 (1.060 g, 0.01 mol) and NaOH (0.160 g, 0.004 mol) were dispersed in 30 mL distilled water. Another solution of $\text{Cu}(\text{NO}_3)_2 \cdot 3\text{H}_2\text{O}$ (1.449 g, 0.006 mol), $\text{Ni}(\text{NO}_3)_2 \cdot 6\text{H}_2\text{O}$ (2.617 g, 0.009 mol), $\text{FeCl}_3 \cdot 6\text{H}_2\text{O}$ (0.811 g, 0.003 mol) and $\text{Cr}(\text{NO}_3)_3 \cdot 9\text{H}_2\text{O}$ (0.800 g, 0.002 mol) in 30 mL distilled water was prepared. Both of the solutions and suspension were sonicated for 30 min and then they were added simultaneously in a drop-wise manner to a round-bottom flask containing stirred distilled water (30 mL). During the progress of the reaction, pH was kept at 11 by addition of suitable amounts of NaOH and HCl solutions. The resulting slurry was stirred for further 30 min at room temperature and was subsequently aged for 20 h at 80 °C. The resulting mixture was cooled to the room temperature and then filtered. After that, the product was dried at 150 °C to afford $\text{Fe}_3\text{O}_4@SiO_2@Cu-Ni-Fe-Cr$ LDH as a solid material of 3.09 g.

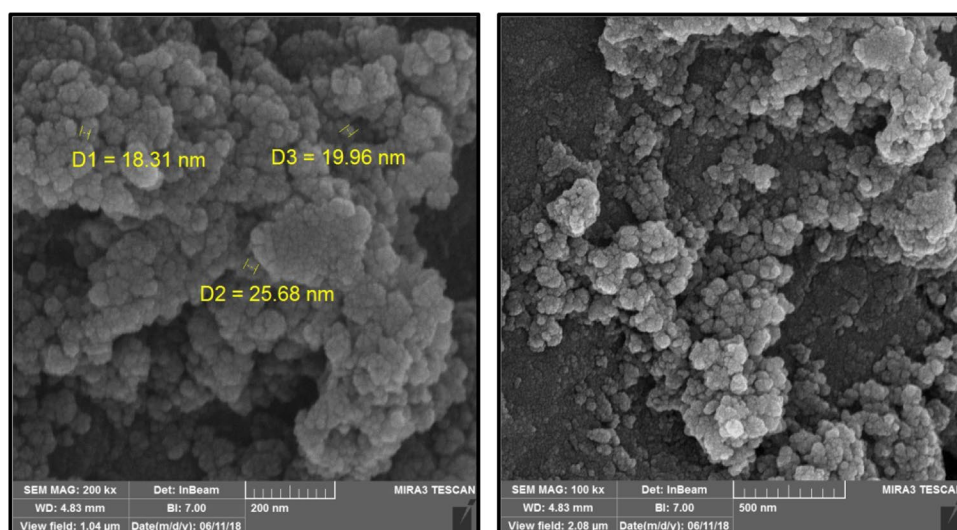
A typical procedure for reduction of nitrobenzene

In a round-bottom flask (10 mL) containing 2 mL water, a mixture of nitrobenzene (0.123 g, 1 mmol) and $\text{Fe}_3\text{O}_4@SiO_2@Cu-Ni-Fe-Cr$ LDH (10 mg) was prepared and the resulting mixture was stirred for 5 min. Next, NaBH_4 (0.076 g, 2 mmol) was added and the reaction mixture was stirred magnetically for 3 min under oil bath conditions (60–70 °C). TLC monitored the progress of the reaction (eluent, *n*-hexane/*EtOAc*: 5/2). After completion of the reduction reaction, the mixture was cooled to the room temperature. *EtOAc* (3 mL) was then added and the resulting mixture was again stirred for 10 min. The magnetic nanocatalyst was separated by an external magnet followed by extraction with *EtOAc* (2 × 5 mL). The combined organic layers were dried over anhydrous Na_2SO_4 . Evaporation of the solvent afforded the pure liquid aniline in 95% yield (Table 2, entry 1).

A typical procedure for reductive-acetylation of nitrobenzene

In a round-bottom flask (10 mL) equipped with a magnetic stirrer, a mixture of nitrobenzene (0.123 g, 1 mmol) and H_2O (2 mL) was prepared. $\text{Fe}_3\text{O}_4@SiO_2@Cu-Ni-Fe-Cr$ LDH (10 mg) was then added and the mixture was stirred for 5 min. Next, NaBH_4 (0.076 g, 2 mmol) was added and the reaction mixture was stirred magnetically for 3 min at 60–70 °C. TLC monitored the progress of the reaction (eluent, *n*-hexane / *EtOAc*: 5/2). Ac_2O (0.102 g, 1 mmol) was then added and the reductive-acetylation was occurred immediately at 60–70 °C. After formation of acetanilide, the core-shell nanocatalyst was separated by an external magnet and the reaction mixture was extracted with *EtOAc* (2 × 5 mL). The organic layer was dried over anhydrous

Fig. 12 FE-SEM image of the recovered $\text{Fe}_3\text{O}_4@\text{SiO}_2@\text{Cu-Ni-Fe-Cr}$ LDH after second run



Na_2SO_4 followed by evaporation of the solvent to afford pure acetanilide in 96% yield (Table 4, entry 1).

Conclusions

In summary, we have introduced a novel, efficient and green catalyst such as mesoporous $\text{Fe}_3\text{O}_4@\text{SiO}_2@\text{Cu-Ni-Fe-Cr}$ LDH and then characterized using FTIR, XRD, SEM, EDX, BET, VSM, TGA, DTG and TEM analyses. This heterogeneous catalyst displayed a significant catalytic activity towards reduction and one-pot reductive-acetylation of nitroarenes with $\text{NaBH}_4/\text{Ac}_2\text{O}$ system as reducing/acetylation agents in water. This procedure has several advantages in terms of mild reaction conditions, high yields, short reaction times, simple workup procedure and reusability of the magnetic LDH nanocatalyst. The catalyst can be reused six times without considerable decrease in activity.

Acknowledgements The authors gratefully acknowledge the financial support of this work by the research council of Urmia University.

References

- M. Boudart, *Chem. Rev.* **95**, 661 (1995)
- N. Mizuno, M. Misono, *Chem. Rev.* **98**, 199 (1998)
- M. Heitbaum, F. Glorius, I. Escher, *Angew. Chem. Int. Ed.* **45**, 4732 (2006)
- S.M. George, *Chem. Rev.* **95**, 475 (1995)
- H. Hattori, *Chem. Rev.* **95**, 537 (1995)
- A. Corma, H. Garcia, F.X. Llabres i Xamena, *Chem. Rev.* **110**, 4606 (2010)
- M. Gilanizadeh, B. Zeynizadeh, *New J. Chem.* **42**, 8553 (2018)
- M.R. Othman, Z. Helwani, W.J.N. Martunus, Fernando, *Appl. Organomet. Chem.* **23**, 335 (2009)
- M.B. Gawande, R.K. Pandey, R.V. Jayaram, *Catal. Sci. Technol.* **2**, 1113 (2012)
- M. Gilanizadeh, B. Zeynizadeh, *Res. Chem. Intermed.* <https://doi.org/10.1007/s11164-018-3475-0> (2018)
- M. Gilanizadeh, B. Zeynizadeh, E. Gholamiyan, Iran. J. Sci. Technol. T. A Sci. <https://doi.org/10.1007/s40995-018-0594-9> (2018)
- R.G. Chaudhuri, S. Paria, *Chem. Rev.* **112**, 2373 (2012)
- V. Polshettiwar, R. Luque, A. Fihri, H. Zhu, M. Bouhrara, J.M. Basset, *Chem. Rev.* **111**, 3036 (2011)
- K. Bakmutsky, N.L. Wieder, M. Cargnello, B. Galloway, P. Fornasiero, R.J. Gorte, *Chem. Sustain. Chem.* **5**, 140 (2012)
- Z. Shu, S. Wang, *J. Nanomater* (2009) <http://dx.doi.org/10.1155/2009/340217>
- F. Niu, L. Zhang, S.Z. Luo, W.G. Song, *Chem. Commun.* **46**, 1109 (2010)
- S. Xuan, W. Jiang, X. Gong, Y. Hu, Z. Chen, *J. Phys. Chem. C* **113**, 553 (2009)
- R. Cano, D.J. Ramon, M. Yus, *J. Org. Chem.* **75**, 3458 (2010)
- M.J. Aliaga, D.J. Ramon, M. Yus, *Org. Biomol. Chem.* **8**, 43 (2010)
- G. A.Uheida, E. Salazar-Alvarez, Z. Bjorkman, M. Yu, Muhammed, *J. Colloid Interface Sci.* **298**, 501 (2006)
- T. Poursaberi, V. Akbar, S.M.R. Shoja, Iran. J. Chem. Chem. Eng. **34**, 41 (2015)
- M. Ma, J. Xie, Y. Zhang, Z. Chen, N. Gu, *Mater. Lett.* **105**, 36 (2013)
- J. Liu, X. Peng, W. Sun, Y. Zhao, C. Xia, *Org. Lett.* **10**, 3933 (2008)
- M. Kotani, T. Koike, K. Yamaguchi, N. Mizuno, *Green Chem.* **8**, 735 (2006)
- K.V.S. Ranganath, J. Kloesges, A.H. Schafer, F. Glorius, *Angew. Chem. Int. Ed.* **49**, 7786 (2010)
- S.T. Chen, R. Si, T. Eric, J. Jonathan, J.Y. Chen, *J. Phys. Chem. C* **116**, 12969 (2012)
- H.D. Cai, K.G. Li, M. Shen, S. Wen, Y. Luo, C. Peng, G. Zhang, X. Shi, *J. Mater. Chem.* **22**, 15110 (2012)
- K.V.S. Ranganath, F. Glorius, *Catal. Sci. Technol.* **1**, 13 (2011)
- Z. Zhao, J. Liu, F. Cui, H. Feng, L. Zhang, *J. Mater. Chem.* **22**, 9052 (2012)
- W. Lu, Y. Shen, A. Xie, X. Zhang, W. Chang, *J. Phys. Chem. C* **114**, 4846 (2010)
- A.M. Tafesh, J. Weiguny, *Chem. Rev.* **96**, 2035 (1996)
- S.A. Lawrence, *Amines: Synthesis, Properties and Applications* (Cambridge University Press, Cambridge, 2004)

33. T.C. Nugent, *Chiral Amine Synthesis: Methods, Developments and Applications* (Wiley, Weinheim, 2010)
34. T. Farooqui, A.A. Farooqui, *Biogenic Amines: Pharmacological, Neurochemical and Molecular Aspects in the CNS* (Nova Science, New York, 2010)
35. A.M. Birch, S. Groombridge, R. Law, A.G. Leach, C.D. Mee, C. Schramm, *J. Med. Chem.* **55**, 3923 (2012)
36. M.R. Yazdanbakhsh, A. Mohammadi, E. Mohajerani, H. Nemati, N.H. Nataj, A. Moheghi, E. Naemikhah, *J. Mol. Liq.* **151**, 107 (2010)
37. S. Vishnoi, V. Agrawal, V.K. Kasana, *J. Agric. Food Chem.* **57**, 3261 (2009)
38. J. Seyden-Penne, *Reductions by the Alumino and Borohydrides in Organic Synthesis*, 2nd edn. (Wiley-VCH, New York, 1997)
39. A.F. Abdel-Magid, *Reductions in Organic Synthesis. ACS Symposium Series*, vol. 641 (1996)
40. P.G. Andersson, I.J. Munslow, *Modern Reduction Methods* (Wiley-VCH, New York, 2008)
41. M. Hudlicky, *Reductions in Organic Chemistry* (Ellis Horwood, Chichester, 1984)
42. P.S. Rathore, R. Patidar, T. Shripathi, S. Thakore, *Catal. Sci. Technol.* **5**, 286 (2015)
43. M.B. Gawande, A.K. Rathi, P.S. Branco, I.D. Nogueira, A. Velhinho, J.J. Shrikhande, U.U. Indulkar, R.V. Jayaram, C.A.A. Ghuman, N. Bundaleski, O.M.N.D. Teodoro, *Chem. Eur. J.* **18**, 12628 (2012)
44. R.K. Rai, A. Mahata, S. Mukhopadhyay, S. Gupta, P.Z. Li, K.T. Nguyen, Y. Zhao, B. Pathak, S.K. Singh, *Inorg. Chem.* **53**, 2904 (2014)
45. R.V. Jagadeesh, D. Banerjee, P.B. Arockiam, H. Junge, K. Junge, M.M. Pohl, J. Radnik, A. Brückner, M. Beller, *Green Chem.* **17**, 898 (2015)
46. B. Zeynizadeh, K. Zahmatkesh, *J. Chin. Chem. Soc.* **50**, 267 (2003)
47. B. Zeynizadeh, M. Zabihzadeh, *J. Iran. Chem. Soc.* **12**, 1221 (2015)
48. M. Periasamy, M. Thirumalaikumar, *J. Organomet. Chem.* **609**, 137 (2000)
49. B.H. Kim, R. Han, F. Piao, Y.M. Jun, W. Baik, B.M. Lee, *Tetrahedron Lett.* **44**, 77 (2003)
50. Y. Jia, Q. Li, X. Wang, H. Wang, X. Liu, *J. Shanghai Univ.(Eng.)* **10**, 277 (2006)
51. X. Wang, H. Guo, G. Xie, Y. Zhang, *Synth. Commun.* **34**, 3001 (2004)
52. D.C. Owsley, J.J. Bloomfield, *Synthesis* 118 (1977)
53. K.Y. Lee, J.M. Kim, J.N. Kim, *Bull. Korean Chem. Soc.* **23**, 1359 (2002)
54. R.N. Baruah, *Indian J. Chem.* **39B**, 300 (2000)
55. A.E. Wahba, J. Peng, M.T. Hamann, *Tetrahedron Lett.* **50**, 3901 (2009)
56. R.J. Rahaim, R.E. Maleczka, *Synthesis* **19**, 3316 (2006)
57. M.L. Kantam, R.S. Reddy, K. Srinivas, R. Chakravarti, B. Sreedhar, F. Figueras, C.V. Reddy, *J. Mol. Catal. A: Chem.* **355**, 96 (2012)
58. E.M. Nahmed, G. Jenner, *Tetrahedron Lett.* **32**, 4917 (1991)
59. B. Zeynizadeh, D. Setamdideh, *Synth. Commun.* **36**, 2699 (2006)
60. B. Zeynizadeh, H. Ghasemi, *J. Chem. Res.* 542 (2006)
61. Z. Shokri, B. Zeynizadeh, S.A. Hosseini, B. Azizi, *J. Iran. Chem. Soc.* **14**, 101 (2017)
62. B. Zeynizadeh, I. Mohammadzadeh, Z. Shokri, S.A. Hosseini, *J. Colloid Interface Sci.* **500**, 285 (2017)
63. Z. Shokri, B. Zeynizadeh, S.A. Hosseini, *J. Colloid Interface Sci.* **485**, 99 (2017)
64. G.Y. Li, Y.R. Jiang, K.L. Huang, P. Ding, L.L. Yao, *Colloids Surf. A* **320**, 11 (2008)
65. J.A. Lopez, F. González, F.A. Bonilla, G. Zambrano, M.E. Gómez, *Rev. Latin Am. Metal. Mat.* **30**, 60 (2010)
66. C. Busetto, G.D. Piero, G. Manara, F. Trifiro, A. Vaccari, *J. Catal.* **85**, 260 (1984)
67. K. Basu, S. Chakraborty, C. Saha, A. Kumar Sarkar, *IOSR J. Appl. Chem.* **7**, 30 (2014)
68. X. Liu, Z. Ma, J. Xing, H. Liu, *J. Magn. Magn. Mater.* **270**, 1 (2004)
69. Y. Zhang, G.M. Zeng, L. Tang, D.L. Huang, X.Y. Jiang, Y.N. Chen, *Biosens. Bioelectron.* **22**, 2121 (2007)

Affiliations

Masumeh Gilanizadeh¹  · Behzad Zeynizadeh¹

✉ Masumeh Gilanizadeh
masumehgilanizadeh@gmail.com

¹ Faculty of Chemistry, Urmia University, Urmia 5756151818, Iran